

Reprinted from

PHYSICS LETTERS A

Physics Letters A 217 (1996) 305-314

An experimental demonstration of resonant sideband extraction for laser-interferometric gravitational wave detectors

G. Heinzel¹, J. Mizuno², R. Schilling, W. Winkler, A. Rüdiger, K. Danzmann³

Max-Planck-Institut für Quantenoptik, Hans-Kopfermann-Strasse 1, D-85748 Garching, Germany

Received 29 February 1996; accepted for publication 30 April 1996

Communicated by P.R. Holland



ELSEVIER

PHYSICS LETTERS A

EDITORS

V.M. Agranovich, Institute of Spectroscopy,
Russian Academy of Sciences,
Troitsk, Moscow obl. 142092, Russian Federation
E-mail: agran@theor.isan.msk.su; Fax: +7 095 3340224
*Condensed matter physics, Theoretical physics, Statistical
properties of condensed matter*

A.R. Bishop, MS-B262, Theoretical Division and Center for
Nonlinear Studies, Los Alamos National Laboratory,
Los Alamos, NM 87545, USA
E-mail: phys_let@tdo-serv.lanl.gov; Fax: +1 505 6653003
Nonlinear science, Condensed matter physics

C.R. Doering, MS-B262, Center for Nonlinear Studies,
Los Alamos National Laboratory, Los Alamos, NM 87545, USA
E-mail: phys_let@tdo-serv.lanl.gov; Fax: +1 505 6652659
Nonlinear science, Statistical physics

J. Flouquet, CRTBT/CNRS, Boîte Postale 166,
F-38042 Grenoble Cedex 9, France
Fax: +33 76 855610
Condensed matter physics

A.P. Fordy, Centre for Nonlinear Studies and Department of
Applied Mathematical Studies, University of Leeds,
Leeds LS2 9JT, UK
E-mail: amt6za@leeds.ac.uk; Fax: +44 113 2429925
Nonlinear science, Mathematical physics

B. Fricke, Fachbereich Physik, Universität Kassel,
Heinrich-Plett-Strasse 40, 34132 Kassel, Germany
E-mail: pla@physik.uni-kassel.de; Fax: +49 561 8044006
Atomic, molecular and cluster physics

P.R. Holland, School of Interdisciplinary Sciences,
University of the West of England, Coldharbour Lane, Frenchay,
Bristol BS16 1QY, UK
E-mail: phys-ldr@uwe.ac.uk; Fax: +44 117 9762502
*General physics, Quantum mechanics, Quantum optics,
Gravitation*

A. Legendijk, Van der Waals-Zeeman Laboratorium,
Universiteit van Amsterdam, Valckenierstraat 65-67,
1018 XE Amsterdam, The Netherlands
E-mail: izwart@phys.uva.nl; Fax: +31 20 5255788
Condensed matter physics, Optical physics

M. Porkolab, Plasma Fusion Center, NW17-288,
Massachusetts Institute of Technology, 175 Albany Street,
Cambridge, MA 02139, USA
E-mail: arlington@pfc.mit.edu; Fax: +1 617 2530238
*Plasma and fluid physics, Statistical properties of plasmas
and fluids*

L.J. Sham, Department of Physics, 0319, University of California,
San Diego, 9500 Gilman Drive, La Jolla, CA 92023-0319, USA
E-mail: lsham@ucsd.edu; Fax: +1 619 4590336
Condensed matter physics

J.P. Vigiér, Laboratoire de Gravitation et Cosmologie Rélativistes,
Université Pierre et Marie Curie, Tour 22-12, 4ème étage,
Boîte 142, 4 Place Jussieu, 75252 Paris Cedex 05, France
Fax: +33 1 40510661
General physics, Quantum mechanics

Aims and scope

Physics Letters A ensures the rapid publication of short communications in all fields of Physics, excluding Nuclear Physics and Particle Physics.

Abstracted/indexed in:

Chemical Abstracts; Current Contents: Physical, Chemical and Earth Sciences; Engineered Materials Abstracts; INSPEC; Metals Abstracts; Physics Briefs

Subscription information 1996

PHYSICS LETTERS A (ISSN 0375-9601) and PHYSICS LETTERS B (ISSN 0370-2693) will each be published weekly. For 1996 13 volumes, volumes 211-223 (78 issues altogether) of Physics Letters A have been announced. For 1996 25 volumes, volumes 365-389 (100 issues altogether) of Physics Letters B have been announced. The subscription prices for these volumes are available upon request from the Publisher. PHYSICS REPORTS (ISSN 0370-1573) will be published approximately weekly. For 1996 13 volumes, volumes 264-276 (78 issues to-

gether) of Physics Reports have been announced. The subscription price for these volumes is available upon request from the Publisher.

A combined subscription to the 1996 issues of Physics Letters A, Physics Letters B and Physics Reports is available at a reduced rate.

Subscriptions are accepted on a prepaid basis only and are entered on a calendar year basis. Issues are sent by SAL (Surface Air Lifted) mail wherever this service is available. Airmail rates are available upon request. Please address all enquiries regarding orders and subscriptions to:

Elsevier Science B.V.
Order Fulfillment Department
P.O. Box 211, 1000 AE Amsterdam
The Netherlands
Tel. + 31 20 4853642, Fax: +31 20 4853598

Claims for issues not received should be made within six months of our publication (mailing) date.

US mailing notice - Physics Letters A (ISSN 0375-9601) is published weekly by Elsevier Science B.V., P.O. Box 211, 1000 AE Amsterdam, The Netherlands. Annual subscription price in the USA is US\$ 3203.00 (valid in North, Central and South America only), including air speed delivery. Second class postage paid at Jamaica, NY 11431.

USA POSTMASTERS: Send address changes to Physics Letters A, Publications Expediting, Inc., 200 Meacham Avenue, Elmont, NY 11003. **AIRFREIGHT AND MAILING** in the USA by Publications Expediting, Inc., 200 Meacham Avenue, Elmont, NY 11003.

⊙ The paper used in this publication meets the requirements of ANSI/NISO Z39.48-1992 (Permanence of Paper).





ELSEVIER

22 July 1996

PHYSICS LETTERS A

Physics Letters A 217 (1996) 305–314

An experimental demonstration of resonant sideband extraction for laser-interferometric gravitational wave detectors

G. Heinzl¹, J. Mizuno², R. Schilling, W. Winkler, A. Rüdiger, K. Danzmann³

Max-Planck-Institut für Quantenoptik, Hans-Kopfermann-Strasse 1, D-85748 Garching, Germany

Received 29 February 1996; accepted for publication 30 April 1996

Communicated by P.R. Holland

Abstract

Resonant sideband extraction is a new optical configuration for laser-interferometric gravitational wave detectors with Fabry–Perot cavities in the arms. It reduces the thermal load on the beam splitter and the coupling mirrors of the cavities and also allows one to adapt the frequency response of the detector to a variety of requirements. We report the first experimental demonstration using a table-top setup at a *detuned* operating point. An increase of sensitivity by 6 dB was observed for artificial signals at frequencies above the arm cavity bandwidth, and the overall transfer function agreed well with theoretical predictions.

PACS: 04.80.Nn; 07.60.Ly; 42.25.Hz; 95.55.Ym

Keywords: Resonant sideband extraction; Michelson interferometer; Fabry–Perot; Mach–Zehnder; Gravitational wave detector; Three-mirror cavity

1. Introduction

Direct detection of gravitational waves by laser interferometry seems possible within the next several years. Construction work has begun for several large detectors (e.g. LIGO in the U.S. [1], VIRGO [2] and GEO600 [3] in Europe, and others). One fundamental limit for the sensitivity of any optical detector is given by the photon counting error (*shot noise*). In order to achieve the desired high sensitivity, various extensions to the basic Michelson interferometer have been proposed, such as delay lines or Fabry–Perot cavities in the arms, power- and signal-recycling [4,5]. It can be shown [6] that for any of these configurations the shot-noise limited sensitivity (expressed as linear spectral density \bar{h} of strain in space producing the same output signal as the intrinsic detector noise) is proportional to $\sqrt{\Delta f_{\text{BW}}/E}$, where E is the amount of light

¹ E-mail: ghh@mpq.mpg.de.

² E-mail: mizuno@mpq.mpg.de.

³ Also at Universität Hannover, Institut für Atom- und Molekülphysik, Appelstrasse 2, D-30167 Hannover, Germany.

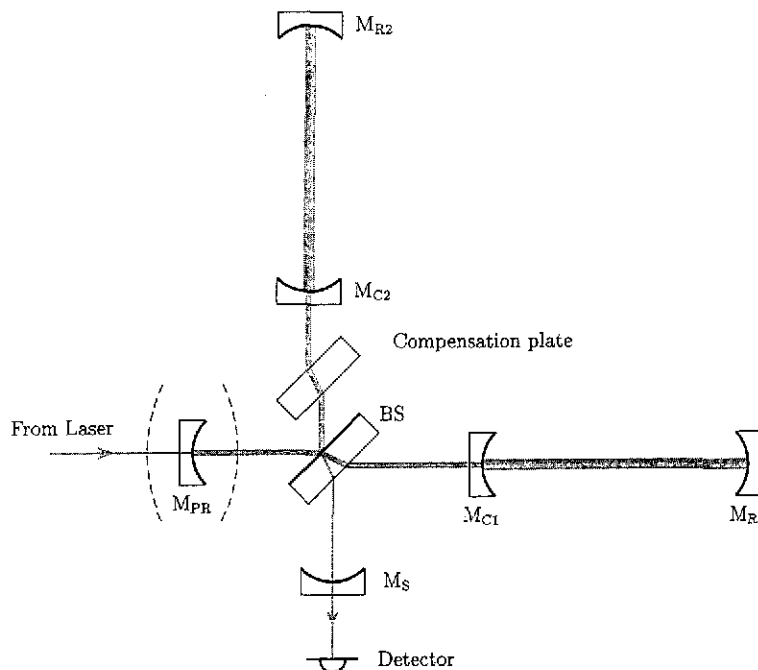


Fig. 1. Optical layout for resonant sideband extraction. Power recycling (with mirror M_{PR}) is an option not affecting the principle of RSE. The compensation plate may be included for reasons of symmetry between the two arms.

energy stored in the arms, and Δf_{BW} the detector bandwidth. All of the above mentioned schemes amount to increasing E for a given physical arm length and laser power and/or modifying the detector bandwidth.

Among these schemes, power recycling is considered indispensable for all of the planned large detectors. The power gain achievable will, however, be limited by imperfect contrast as well as losses in the substrates of the beam splitter (and those of the arm cavity coupling mirrors). Furthermore, the high-power beam may cause absorption-induced thermal lensing and birefringence in the substrates [7–9].

By using high-finesse Fabry–Perot arm cavities, the high-power beam is confined to within the arm cavities and is not transmitted through any substrate. The usable finesse of the arm cavities was, however, believed to be limited by the required detector bandwidth.

Resonant sideband extraction (RSE) [6,10] was proposed as a new optical configuration to overcome this limitation. In particular, the detector bandwidth can be made broader than the arm-cavity bandwidth, thereby permitting the use of high-finesse cavities in the arms. There exist non-detuned and detuned modes of operation, where “tuned” in this paper refers to making the signal extraction cavity resonant for the carrier, which yields the broadest possible detector bandwidth. The “detuned” modes permit a sensitivity peak to be obtained at an adjustable frequency.

The outline of this paper is as follows: In Section 2, we describe the frequency response of RSE, closely following Ref. [6]. Our experimental setup is described in Section 3. The results are discussed in Section 4.

2. Frequency response of resonant sideband extraction

Fig. 1 shows the basic optical layout for RSE. It resembles that of signal recycling with Fabry–Perot cavities in the arms, but here a different sub-wavelength positioning of the signal extraction mirror (M_S in Fig. 1)

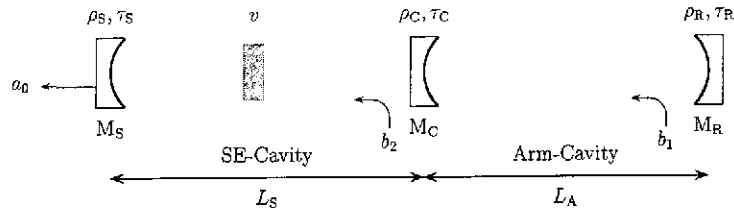


Fig. 2. Three-mirror cavity storing the signal sidebands.

produces a different effect, as described below.

To simplify the analysis, we assume all interfering beams to have the same polarization and transverse mode structure. To compute the frequency response, we also assume a 50/50 beam splitter, both arm cavities to be identical and in resonance with the incoming light of angular frequency ω_0 (the “carrier”). Furthermore, we assume the interferometer to be operated at a dark fringe (at the detector port), i.e. all carrier light returning from the arms is interfering constructively towards the laser (or power-recycling mirror). Note that the amplitude reflectivity of the Michelson interferometer as a whole seen from either port is identical (if the beam splitter’s transmittance equals its reflectivity), whatever the arms are.

A suitably oriented and polarized gravitational wave produces a phase modulation of opposite sign in the two arms. In the following we consider only a single frequency component of angular frequency ω_g . The phase modulation sidebands at $\omega_0 \pm \omega_g$ interfere constructively towards the signal extraction mirror M_S . After being reflected by M_S , they re-enter the interferometer, which in turn reflects them back to M_S . The signal sidebands are thus stored in a “split” cavity [11] composed of the Michelson interferometer and M_S . Under the above assumptions, this split cavity is equivalent to a *three-mirror cavity* (Fig. 2) formed by M_S , M_C and M_R , where the two identical arm cavities have been “folded” together to form a single cavity consisting of M_C and M_R . (The notations in Fig. 2 are explained in the context of Eqs. (1) and (2)).

One possible interpretation of this three-mirror cavity is to consider the cavity as being composed of M_R and a *compound mirror* formed by M_S and M_C . The compound mirror (which we also call the “signal extraction cavity”) has frequency-dependent transmittance and reflectivity. In *signal recycling*, this cavity is tuned to “anti-resonance” (i.e. centered between two successive resonances) so as to obtain a *lower* transmittance than that of M_C alone, resulting in an *increased* storage time for the signal.

The purpose of RSE, on the other hand, is to *reduce* the storage time for the signal, in order to allow long storage times for the carrier without sacrificing detector bandwidth. This can be achieved by tuning the signal extraction cavity to resonance so that its transmittance for the signal frequencies of interest is *higher* than that of M_C alone. For these frequencies the storage time in the three-mirror cavity is shorter than that in the unmodified arm cavity. In the non-detuned case, this reduction of the storage time results in an increased bandwidth.

To compute the frequency response we consider the light amplitudes going to and from each mirror in the scalar model (see Fig. 2). As input to the cavity we have b_1 , which represents the signal sidebands produced by differential phase modulation of the carrier (e.g. by gravitational waves) in the arms. Of importance in our experiment is also a further input b_2 , which corresponds to phase modulation sidebands produced between the beam splitter and arm cavity. Note that the carrier (in an ideal dark-fringe operation) never reaches M_S and therefore is not considered in this picture.

The amplitudes at the different points are coupled by a set of linear equations. Solving this set for the output amplitude a_0 yields the transfer functions

$$G_1(\omega, \delta) = \frac{a_0}{b_1} = \frac{\tau_C \tau_S v e^{i\omega(T_A + T_S)}}{1 - \rho_R \rho_C e^{2i\omega T_A} - \rho_C \rho_S v^2 e^{i(2\omega T_S + \delta)} + \rho_R \rho_S v^2 e^{i(2\omega(T_A + T_S) + \delta)}}, \quad (1)$$

for signals fed into the arm cavity (setting $b_2 = 0$), and

$$G_2(\omega, \delta) = \frac{a_0}{b_2} = \frac{\tau_S v e^{i\omega T_S} (1 - \rho_R \rho_C e^{2i\omega T_A})}{1 - \rho_R \rho_C e^{2i\omega T_A} - \rho_C \rho_S v^2 e^{i(2\omega T_S + \delta)} + \rho_R \rho_S v^2 e^{i[2\omega(T_A + T_S) + \delta]}} \quad (2)$$

for signals fed into the signal extraction cavity (setting $b_1 = 0$). Here τ and ρ denote the amplitude transmission and reflection coefficients of the respective mirrors. The angular frequency ω denotes the light frequency offset with respect to the carrier frequency (thus $\omega = \pm\omega_g$ for the upper and lower sideband, respectively). The phase δ represents the detuning of the signal extraction cavity, with $\delta = 0$ for non-detuned (broadband) RSE, $\delta = \pi$ for signal recycling and all other values representing detuned cases. $T_S = L_S/c$ and $T_A = L_A/c$ are the one-way light travel times in the signal extraction cavity and arm cavity, respectively. The losses of the arm cavity are modeled by a finite transmittance of the rear mirror $0 < \tau_R^2 \ll 1$, and the losses in the signal extraction cavity (beam splitter, imperfect contrast, etc.) by an amplitude transmittance $v \lesssim 1$. If the signal is a true gravitational wave acting on the whole length of the cavity, G_1 must be multiplied by the factor $\sin(\omega T_A)/\omega T_A$ (see e.g. Ref. [12]), which can however be neglected for our experiment.

We use external modulation (see e.g. Ref. [13] and references therein) to detect the signal sidebands in our experiment. In the Mach–Zehnder interferometer used for this purpose, the light eventually leaving the Michelson interferometer through M_S , with amplitude a_s , is superimposed with a reference beam that has been phase modulated at an angular frequency ω_e . A relative phase shift ψ is introduced between signal and reference beam before they are superimposed in order to adjust for maximum output signal. Synchronous demodulation of the resulting photocurrent at the modulation frequency ω_e produces an output signal given by

$$y = y_0 [\operatorname{Re}(a_s) \sin \psi + \operatorname{Im}(a_s) \cos \psi] = y_0 \operatorname{Im}(a_s e^{i\psi}) \quad (3)$$

where all constant factors have been included in y_0 .

The signal wave a_s consists of two sidebands a_+ and a_- , which are not necessarily symmetric in the detuned cases of RSE (or signal recycling),

$$a_s = i a_+ e^{i\omega_g t} + i a_- e^{-i\omega_g t} \quad (4)$$

The factors i arise from setting the carrier phase to zero. For the output signal as detected by external modulation we get from Eqs. (3) and (4),

$$y = \operatorname{Re}(A e^{i\omega_g t}), \quad \text{with } A = a_+ e^{i\psi} + a_-^* e^{-i\psi} \quad (5)$$

where A represents the complex amplitude of the output signal of frequency ω_g [6]. The asterisk denotes complex conjugation.

Thus the transfer function of the interferometer up to the demodulated detector output for phase modulation signals of frequency ω_g generated inside either the arm cavity or signal extraction cavity is given (neglecting common constant factors) by

$$H_1(\omega_g, \delta, \psi) = G_1(\omega_g, \delta) e^{i\psi} + G_1^*(-\omega_g, \delta) e^{-i\psi} \quad (6)$$

$$H_2(\omega_g, \delta, \psi) = G_2(\omega_g, \delta) e^{i\psi} + G_2^*(-\omega_g, \delta) e^{-i\psi} \quad (7)$$

since both sidebands have been produced with the same amplitude by the phase modulation.

Note that the transfer function of the interferometer depends on ψ , the relative phase between signal wave and reference wave. This becomes important in detuned cases of RSE (or signal recycling), where both sidebands will generally have different amplitudes. One extreme is the “single sideband” case, where the signal wave a_s is dominated by only one of the two sidebands. This approximately happens near the sensitivity peak of a detuned interferometer. Then the dependence on ψ is small, as can be seen from Eq. (5) by setting $a_- = 0$.

When the two sidebands have comparable amplitudes, however, the amount of detected output signal depends sinusoidally on ψ . It turns out that there is not one fixed optimum detection phase ψ for all signal frequencies

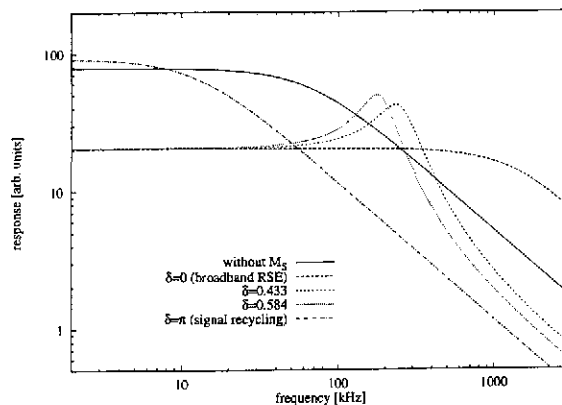


Fig. 3. Calculated frequency response of our table-top interferometer.

simultaneously. The difference between the optimum ψ for low and for high frequencies (in relation to the peak frequency) is roughly $\pi/2$.

Fig. 3 shows the computed frequency response $|H_1(\omega, \delta, \psi = 0)|$ of our table-top interferometer, using the parameters given in the next section. We have plotted the responses for the non-detuned cases of RSE and signal recycling ($\delta = 0$ and $\delta = \pi$, respectively), two detuned operating points used in our experiment, and the response without any mirror M_5 for comparison. For a clear experimental demonstration of an *increase* in sensitivity we chose the detuned operating points, since test signals were applied by a PZT having a few 100 kHz bandwidth at most. Furthermore, the characteristic peaks in the frequency response allow a better comparison with theory. In order to eliminate the effect of PZT resonances we compared the response with M_5 locked to its proper position to the response with M_5 -removed.

3. Experiment

In our experiment (Fig. 4), the interferometer was illuminated by approximately 300 mW of single-mode light at 514.5 nm from an INNOVA-90 Ar⁺ Laser through two Faraday isolators (made by Optics for Research). Its frequency can be controlled by an intra-cavity Pockels cell and a slow PZT shifting one mirror. The light is phase modulated at 12 MHz by a Gsänger PM-25 Pockels cell PC1, with a modulation index of approximately 0.25 rad. The arm cavities (length 40 cm) consist of flat coupling mirrors (M_{C1} and M_{C2}) with 1850 ppm power transmittance (measured average), and curved reflectors (M_{R1} and M_{R2} , $R = 1$ m) mounted on massive aluminum cylinders. Total cavity losses (excluding τ_C^2) were measured as 350 ppm (the main loss originating from the coating of the rear reflecting mirrors), yielding a finesse of approximately 3000 and a power reflectivity of the cavities of about 50% at resonance. With two mode-matching lenses, more than 90% of the incoming power was coupled into the cavity's fundamental mode.

Glass plates (BP1 and BP2) mounted almost under the Brewster angle reflect 0.5% of the light power returning from the cavities to the photodetectors PD1 and PD2. Their photocurrents are demodulated at 12 MHz and used for stabilization of the laser frequency and the second cavity's length, employing the Pound-Drever method [14]. The system was operated in air and thus very sensitive to acoustic disturbances, necessitating high gain and broad bandwidth for those loops. The first loop (with PD1) locks the laser to the first cavity with a unity-gain frequency of approximately 120 kHz. The second loop (with PD2) locks the length of the second cavity to the laser by adjusting the cavity's length with one slow high-efficiency and one fast PZT, the latter being mounted on an acoustic delay line to reduce low-frequency mechanical resonances. This loop had a unity gain frequency of approximately 40 kHz.

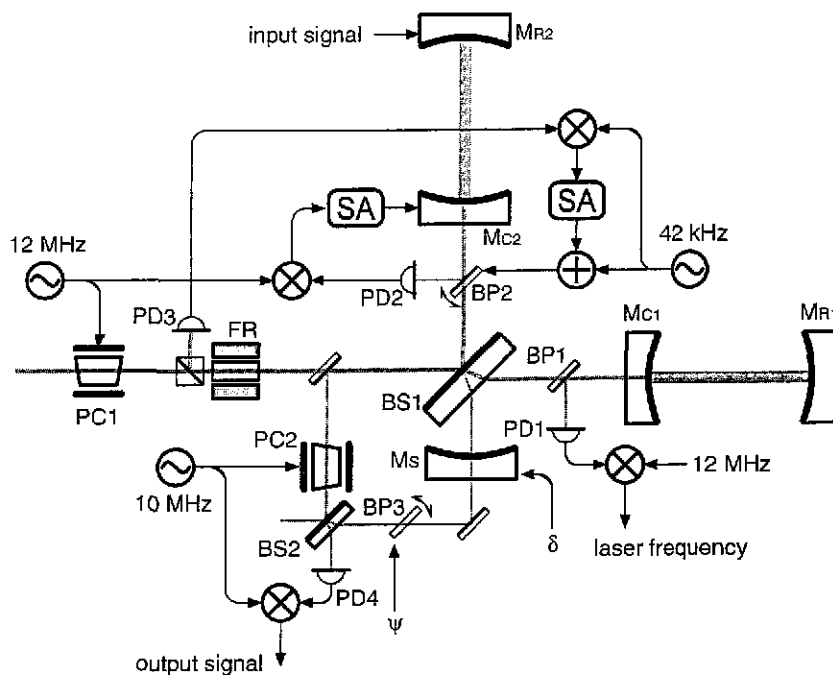


Fig. 4. Simplified diagram of our experimental setup, showing only the control loops for the arm cavities and the Michelson interferometer. FR is a Faraday rotator, PC are Pockels cells, \ominus , \oplus and \otimes electronic oscillators, adders and mixers respectively, BS are beam splitters, BP are glass plates in or near the Brewster angle, PD photodiodes and SA servo amplifiers. See also Fig. 5.

A phase modulation of 42 kHz (*internal modulation*) was applied between the beam splitter and the second cavity by dithering the Brewster plate BP2, which was mounted on a galvanometer scanner allowing tilting about small angles. A tilt of 0.03° was sufficient to change the optical path length by $\lambda/2$, and the modulation index at 42 kHz was approximately 5 mrad. The light returning towards the laser was directed onto photodiode PD3 by one of the Faraday isolators. The photocurrent was demodulated at 42 kHz and fed back to BP2 through an appropriate filter in order to lock the Michelson interferometer to a dark fringe at its output. The unity-gain frequency of this loop was approximately 700 Hz. Another purpose of this 42 kHz modulation is to continually adjust the external modulation's phase relationship, as described below. With both arm cavities locked, the interference minimum was approximately 1% of the power at the maximum.

Test signals up to 500 kHz were fed into the interferometer at the fast PZT holding MR2. This phase modulation in only one arm can be separated into two components of equal magnitude, a common mode component directed towards the laser, and a differential component, which represents the signal of interest. The reference beam for the external modulation was taken from the light returning towards the laser and was phase modulated at 10 MHz ($= \omega_e/2\pi$) by another PM-25 Pockels cell (PC2 in Fig. 4). The relative phase ψ between signal and reference beam was introduced via another galvanometer-tilted Brewster plate BP3. After synchronous demodulation (at 10 MHz), the photocurrent of photodiode PD4 represents the interferometer's output signal.

The phase ψ was controlled so as to maximize the amplitude of the 42 kHz component in the output signal originating from the phase modulation at BP2. The amplitude at 42 kHz was detected by synchronous demodulation of the interferometer output at 42 kHz. This amplitude was maximized by dithering ψ with 260 Hz, demodulating the 42 kHz amplitude at 260 Hz and feeding back the resulting error signal to BP3 through an appropriate loop filter. This loop is not shown in Figs. 4 and 5.